# Spatial Kerr soliton collisions at arbitrary angles

P. Chamorro-Posada and G. S. McDonald*

*Departamento de Teoría de la Señal y Comunicaciones e Ingeniería Telemática, Universidad de Valladolid, ETSI Telecomunicación, Campus Miguel Delibes s/n, 47011 Valladolid, Spain*

(Received 5 June 2005; revised manuscript received 29 July 2006; published 13 September 2006)

The theory of spatial Kerr solitons is extended to colliding beams that are neither almost-exactly copropagating nor almost-exactly counterpropagating. Our new Helmholtz formalism yields results that are consistent with the inherent symmetry of the collision process and that are not predicted by existing paraxial descriptions. Full numerical and approximate analytical results are presented. These show excellent agreement. In particular, Kerr solitons are found to be remarkably robust under nonparaxial collisions.

DOI: 10.1103/PhysRevE.74.036609 PACS number(s): 42.65.Tg, 05.45.Yv

Solitons are universal entities in nonlinear science and their interactions are a key defining property. Understanding soliton collisions is both of fundamental interest and of importance to a wealth of phenomena and proposed applications. In particular, spatial Kerr solitons have attracted extensive experimental and theoretical study in photonics, where multiplexed optical fields may lie at the heart of future technologies [1]. Three distinct angular regimes can be identified for spatial soliton collisions, corresponding to when interacting beams are (i) almost exactly copropagating, (ii) almost exactly counterpropagating, and (iii) at some intermediate angle. The nonlinear Schrödinger (NLS) equation has been the basic model for describing the first regime [2,3], and a recent work [4] has considered regime (ii). However, the inherent spatial-symmetry-breaking assumption of paraxiality means that these existing frameworks can only accurately describe beams aligned at vanishingly small angles with respect to a reference direction.

In this paper, we extend the theoretical description of spatial Kerr soliton collisions to include arbitrary angles and demonstrate excellent agreement between full numerical and analytical predictions. We generally consider angles in unscaled coordinates (i.e., the physical/laboratory angles of the beams). It may be thought that numerous previous works have studied Kerr soliton collisions at low or moderate angles, but this would be a misinterpretation arising from results that are presented in scaled coordinates. For example, Ref. [4] shows beams interacting at an angle of 26.5° (in scaled units). However, the authors of this paper also correctly state that their paraxial model constrains the collision angle in dimensional units to be very small and that beams actually propagate at tiny angles ($0<\theta\ll 1$) with respect to a reference axis.

The nonparaxial nonlinear Schrödinger equation

$$\kappa\frac{\partial^2 u}{\partial\zeta^2}+i\frac{\partial u}{\partial\zeta}+\frac{1}{2}\frac{\partial^2 u}{\partial\xi^2}+|u|^2u=0 \tag{1}$$

is fully equivalent to a nonlinear Helmholtz (NLH) equation [5] and accurately describes the evolution of the complex scalar field of a sufficiently broad beam in a planar Kerr medium. The space coordinates $(z,x)$ are scaled as $\zeta=z/L_D$ and $\xi=\sqrt{2}x/w_0$, where $L_D=kw_0^2/2$ is the diffraction length of a Gaussian beam with waist $w_0$, and $\kappa=1/(k^2w_0^2)=(\lambda/w_0)^2/(4\pi^2n_0^2)$, $u$ is the (TE) normalized electric field, $E(x,z)=E_0u(x,z)\exp(ikz)$, $k=2\pi n_0/\lambda$, $n_0$ is the linear refractive index, $\lambda$ is wavelength, $E_0=[n_0/(kL_Dn_2)]^{1/2}$, and $n_2$ is the Kerr coefficient.

Equation (1) has an exact bright soliton solution [6,7]

$$u(\xi,\zeta)=\eta\,\mathrm{sech}\left[\frac{\eta(\xi+V\zeta)}{\sqrt{1+2\kappa V^2}}\right]\times\exp\left[i\frac{\sqrt{1+2\kappa\eta^2}}{2\kappa}\left(\frac{-2\kappa V\xi+\zeta}{\sqrt{1+2\kappa V^2}}\right)\right]\exp\left(-i\frac{\zeta}{2\kappa}\right), \tag{2}$$

describing a spatial beam propagating at an angle (in unscaled coordinates) of $\theta=\tan^{-1}(\sqrt{2\kappa}V)$ to the longitudinal reference direction. $\eta$ and $V$ are, respectively, the soliton amplitude and transverse velocity parameters. The defocusing Kerr NLH equation has also recently been shown to have a Helmholtz soliton solution [8].

The interpretation of the word "nonparaxial" is commonly oversimplified to imply only narrow-beam nonparaxiality [9–12]. In fact, "nonparaxial" means "not paraxial," i.e., without the paraxial approximation. In this paper, we present precise definitions of three distinct types of nonparaxiality, along with their individual physical correspondences and their relation to the general paraxial approximation. It is well known that narrow-beam effects involve additional considerations (e.g., vectorial effects) in the modeling, but one can clearly distinguish narrow-beam nonparaxiality from Helmholtz-type nonparaxiality. Moreover, a rigorous mathematical argument can support this distinction through precise quantification of the degree of Helmholtz-type nonparaxiality through the magnitude of the angle $\theta$.

The identity relating $\theta$ to velocity $V$ proves that the Helmholtz correction $2\kappa V^2$, appearing in the exact analytical solution (2), may assume arbitrary large values for obliquely propagating beams. Firstly, this verifies that Helmholtz nonparaxiality is highly significant for such broad scalar beams. Secondly, this proves that the commonly used mathematical

*Joule Physics Laboratory, School of Computing, Science and Engineering, Institute for Materials Research, University of Salford, Salford M5 4WT, United Kingdom.

 

basis for narrow-beam nonparaxiality (where $\kappa$ is the single, narrow-beam, order-of-magnitude parameter) is strictly invalid in this angular regime. These observations lend weight to the technical soundness of our approach. They also overturn a growing misconception, that has become rooted during the last three decades [13], that nonparaxiality implies narrow beams and that its analysis needs to be consistent with results from single ($\kappa$) parameter expansion approaches.

The corresponding NLS solitons are recovered when an appropriate multiple limit is enforced. For solution (2), one requires $\kappa \to 0$ (beam not too narrow), $\kappa\eta^2 \to 0$ (beam not too intense), and $\kappa V^2 \to 0$ (propagation angle not too large). These individual conditions are simultaneously required in the paraxial approximation that is captured by the single limit $\kappa|\partial_{\zeta\zeta} u| \to 0$. The nonparaxial term $\kappa\partial_{\zeta\zeta} u$ may thus contribute to distinct nonparaxial scenarios, such as during intense self-focusing [14] or when propagating beams deviate significantly from the axial direction. The former context can lead to beam narrowing that entails more involved field descriptions [14–16]. The latter context introduces a Helmholtz type of nonparaxiality for which Eq. (1) is an adequate model [8].

Equation (1) preserves the rotational symmetry of the wave propagation problem, whereby there is no physical distinction between the space coordinates [5]. A single Helmholtz soliton can thus be propagating at an arbitrary angle $\theta$. The fully second-order NLH equation can also describe the behavior of multiple soliton beams that propagate simultaneously in arbitrary directions.

Here, we consider two such beams, $u_1(\xi,\zeta)$ and $u_2(\xi,\zeta)$. Without loss of generality, we assume they are launched at angles $\theta$ and $-\theta$, respectively, and set $u(\xi,\zeta)=u_1(\xi,\zeta)+u_2(\xi,\zeta)$ in Eq. (1). These beams modulate the refractive index of the Kerr medium according to $|u|^2=|u_1|^2+|u_2|^2+u_1u_2^*+u_2u_1^*$. The last two terms define a real grating that is superimposed on the refractive-index variations due to the individual intensities of the solitons. The grating can result in both enhancement of cross-phase modulation (XPM) and the existence of phase-sensitive terms. To describe the full range of coherence, a grating factor $h$ is introduced and the total XPM contributions are expressed as $(1+h)|u_{3-j}|^2u_j$, where $j=1,2$. The grating parameter has limits $h=0$ and $h=1$ for incoherent and coherent interactions, respectively.

For intermediate interaction angles, phase-sensitive terms can be neglected in the analysis. The interaction is then intensity-driven and governed by coupled equations

$$\kappa\frac{\partial^2 u_j}{\partial\zeta^2} + i\frac{\partial u_j}{\partial\zeta} + \frac{1}{2}\frac{\partial^2 u_j}{\partial\xi^2} + (|u_j|^2 + (1+h)|u_{3-j}|^2)u_j = 0. \quad (3)$$

Since we are considering relatively broad beams, the associated narrow angular spectra imply that the neglected terms would have resonance, i.e., have contribution to Eq. (3), in the case of vanishingly small angles of interaction. Thus, the classification of "intermediate interaction angles" refers to all angular geometries except those of paraxial interactions. Soliton collisions induce a trajectory phase shift $\Delta_j$, for each participating beam, as depicted in Fig. 1 and as described by Eq. (3). In the symmetric-interaction reference frame, specified above, $|\Delta_1|=|\Delta_2|=|\Delta|$. The NLS equation predicts a monotonically decreasing $|\Delta|$ with increasing angle [17], in disagreement with the symmetry of collisions described by Eq. (3).

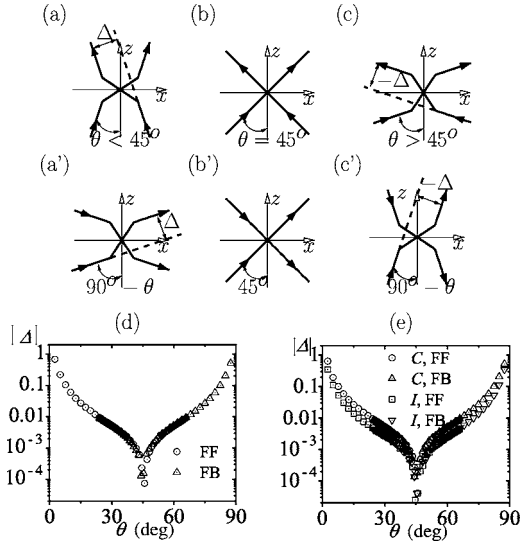


FIG. 1. Geometry of Helmholtz soliton collisions dominated by the individual beam intensities. (a) to (c) correspond to the FF configuration and (a') to (c') to the FB configuration. Magnitude of the trajectory phase shift obtained from the numerical integration of (d) Eq. (1) and (e) Eq. (3) for coherent (C) and incoherent (I) cases for $\kappa=0.001$.

Figures 1(a)–1(c') illustrate the intrinsic symmetry of the collision process governed by Eq. (3). Solid lines sketch typical colliding soliton paths and dashed lines trace paths of the corresponding unperturbed solitons; these paths define a trajectory phase shift in each case. The arrows, superimposed on each solid line, show the directions of the soliton beams. Three novel properties can be highlighted: (i) for intensity-driven collisions such as those described by Eq. (3), if negligible radiation is produced then the graph obtained by reversing the direction arrows of one or both solitons must describe another valid soliton collision geometry; (ii) When $\theta=45°$, $\Delta$ must then vanish on symmetry grounds. Physically, since no net transverse perturbation acts on either soliton, the soliton trajectories are two perpendicular straight lines. (iii) The rotational invariance of the NLH equations can translate into rotational invariance of soliton collision geometries. A case of $\theta<45°$ is shown in Fig. 1(a). Property (ii) is illustrated in Fig. 1(b), where $\theta=45°$. For $\theta>45°$, one can rotate Fig. 1(a) by 90° to obtain Fig. 1(a'). Then, reversal of the propagation direction of one of the solitons gives the configuration shown in Fig. 1(c). The latter operation results in a change in sign of $\Delta$. Similar reasoning permits one to construct the geometries shown in Figs. 1(c') and 1(b').

We denote as FF those configurations of two forward (copropagating) beams, such as those shown in Figs. 1(a)–1(c). Each configuration of copropagation can thus be rotated by 90° to describe an interaction of forward and backward beams (denoted FB). For cases (a)–(c), there is correspondence in the pairs (a,c'), (b,b'), and (c,a'). Identification of this symmetry permits alternative approaches to the

computer simulation of intermediate-angle interactions. Since the NLH equation supports both forward and backward solution components, an initial condition for numerical integration may contain an input soliton (propagating in the forward direction) along with an output soliton (resulting from propagation in the backward direction). For example, if a collision involves negligible radiation, which we find generally true in the intermediate-angle regime, a valid copropagating solution can be obtained by rotating the counterpropagating solution by 90°.

The mathematical and physical properties of the NLH equation are retained in the numerical algorithm [18] we use to solve Eq. (1). Figures 1(d) and 1(e) show the magnitude of the trajectory phase shift obtained from solutions of Eqs. (1) and (3) for both coherent and incoherent regimes of FF and FB configurations. All numerical results are found to reproduce the required symmetry of the problem, and confirm the validity of the 90° rotational equivalence, over a wide angular range. The values of $\Delta$ were obtained by fitting each numerical solution to a pair of hyperbolic secant beams, before and after the collision, to locate the soliton centers. The trajectory phase shifts $\Delta$ were then calculated from the soliton shifts in the $\xi$ direction $\Delta_\xi$ using $\Delta=\Delta_\xi \cos\theta$, where $\cos\theta=1/\sqrt{1+2\kappa V^2}$.

The NLS equation predicts that two equal-amplitude soliton beams with opposite transverse velocities emerge from the collisions studied here. Numerical solution of the NLH equation (1) reveals that amplitudes and widths may undergo small reshaping oscillations, similar to those seen in perturbed single-soliton initial-value problems [7]. Reshaping is accompanied by a small shedding of radiation that only becomes significant in small (paraxial) ranges of collision angles (i.e., for both copropagating and counterpropagating colliding solitons). This radiation phenomenon is typical of soliton interactions in nonintegrable systems, such as the equations describing coherent collisions of almost-exactly counterpropagating solitons [4]. For nonparaxial angles, collisions are remarkably close to elastic, even in the presence of strong longitudinal and transverse gratings. The existence of radiation is of qualitative importance as it indicates the absence of an exact two-soliton solution and the nonintegrability of the NLH equation. The lack of such a NLH multisoliton solution was suggested in Ref. [19]. We note that Hirota's method also fails to find this solution.

An alternative analytical basis has thus been developed for studying intermediate-angle collisions. Our approach is based on an adiabatic perturbation method [19] that exploits the exact Helmholtz one-soliton solution (2). It proves convenient to work within a framework where rotational symmetry is explicitly restored. A suitable NLH equation is found from Eq. (3) by writing $u_j=u_j'\exp(-i\zeta/2\kappa)$ and $\zeta=\sqrt{2\kappa}\zeta'$ to give

$$\frac{1}{2}\frac{\partial^2 u_j}{\partial\zeta^2}+\frac{1}{2}\frac{\partial^2 u_j}{\partial\xi^2}+\frac{1}{4\kappa}u_j+|u_j|^2u_j=R_j[u_j,u_{3-j}], \tag{4}$$

where $R[u_j,u_{3-j}]=-(1+h)|u_{3-j}|^2u_j$, and primes have been dropped for simplicity. In the absence of perturbations, $R_j=0$, Eq. (4) have the exact bright soliton solutions

$$u_j(\xi,\zeta)=\eta_j\,\mathrm{sech}[\eta_j(\xi\cos\theta_j+\zeta\sin\theta_j)]\times\exp\left[i\sqrt{\frac{1+2\kappa\eta_j^2}{2\kappa}}(-\xi\sin\theta_j+\zeta\cos\theta_j)\right]. \tag{5}$$

Substituting $u_j(\xi,\zeta)=\rho_j(\xi,\zeta)\exp[i\phi_j(\xi,\zeta)]$ in Eq. (4), one obtains $\nabla\cdot\mathbf{p}_j=0$, where $\mathbf{p}_j=\frac{1}{2}\rho_j^2\nabla\phi_j$ and $\nabla\equiv(\partial_\zeta,\partial_\xi)$. Integrating over the transverse coordinate $\xi$ gives a statement of conservation of energy flow in the $\zeta$ direction [6,7]: $d_\zeta P_j=0$, where $P_j=\int_{-\infty}^{+\infty}d\xi\frac{1}{2}\rho_j^2\partial_\zeta\phi_j$. For each soliton, $P_j=\eta_j(1+2\kappa\eta_j^2)^{1/2}/(2\kappa)^{1/2}$ and is independent of the propagation direction. Introduction of a perturbation, $R_j\neq 0$, of the type discussed above, does not alter the total beam energy flow. One finds that $d_\zeta P_j=\int_{-\infty}^{+\infty}d\xi\,\mathrm{Im}[R_j\exp(-i\phi_j)]=0$ for XPM-driven interactions. In the paraxial case, the first invariant of the NLS equation gives, within a similar calculation, the condition $d_\zeta\eta_j=0$. It is important to note that this is not the case for the NLH equation, since conservation of the energy flow does not guarantee nonevolving soliton amplitudes and widths.

For $R_j=0$, Eq. (4) can be derived from the Lagrangian densities

$$L_j=\frac{1}{2}\left|\frac{\partial u_j}{\partial\zeta}\right|^2+\frac{1}{2}\left|\frac{\partial u_j}{\partial\xi}\right|^2-\frac{1}{4\kappa}|u_j|^2-\frac{1}{2}|u_j|^4 \tag{6}$$

and this provides two divergence relations

$$\frac{\partial m_{qj}}{\partial\zeta}+\frac{\partial J_{qj}}{\partial\xi}=0,\quad q=\xi,\zeta. \tag{7}$$

Equation (7) may be regarded as a pair of continuity equations. These relations exhibit the required symmetry of invariance under $\xi\leftrightarrow\zeta$. Considering $\zeta$ as the evolution coordinate, the conserved densities are $m_{\xi j}=\frac{1}{2}(\partial_\xi u_j^*\partial_\zeta u_j+\partial_\zeta u_j^*\partial_\xi u_j)$ and $m_{\zeta j}=\frac{1}{2}(|\partial_\zeta u_j|^2-|\partial_\xi u_j|^2)+\frac{1}{2}|u_j|^4+\frac{1}{4\kappa}|u_j|^2$, while the associated currents are $J_{\xi j}=\frac{1}{2}(|\partial_\xi u_j|^2-|\partial_\zeta u_j|^2)+\frac{1}{2}|u_j|^4+\frac{1}{4\kappa}|u_j|^2$ and $J_{\zeta_j}=m_{\xi_j}$. This gives a pair of propagation invariants, $M_{\xi j}=\int_{-\infty}^{+\infty}d\xi m_{\xi j}$ and $M_{\zeta j}=\int_{-\infty}^{+\infty}d\xi m_{\zeta j}$, that define a soliton vector $(M_{\xi j},M_{\zeta j})=\eta_j(3+4\kappa\eta_j^2)/(3\kappa)(-\sin\theta_j,\cos\theta_j)$.

Using the perturbed system (4), one can obtain a set of four equations of motion:

$$\frac{dM_{qj}}{d\zeta}=2\int_{-\infty}^{+\infty}d\xi\,\mathrm{Re}\left[R_j^*\frac{\partial u_j}{\partial q}\right],\quad j=1,2;\ q=\xi,\zeta. \tag{8}$$

In order to quantify how soliton $3-j$ influences the evolution of soliton $j$, approximate analytical results are derived. New coordinates are introduced that have an evolution variable $s$ along the initial propagation direction of soliton $j$, and perturbations to this soliton are quantified in a dimension $t$ transverse to $s$. The angular deviation of the soliton is assumed to be sufficiently small, $\delta\theta_j(s)\leqslant O(\kappa)$, that an appropriate ansatz is

$$u_j(t,s) = a_j \,\mathrm{sech}[b_j(t+t_{0j})]\exp[i\phi_{0j}(-\delta\theta_j(t+t_{0j})+\sigma_j)]. \tag{9}$$

The parameters $a_j(s)=\eta_{0j}+\delta a_j(s)$, $b_j(s)=\eta_{0j}+\delta b_j(s)$, $t_{0j}(s)$, and $\sigma_j(s)=s+\delta\sigma_j(s)$ give the amplitude, inverse width, position and phase variation along the soliton center, respectively, and $dt_{0j}/ds=\delta\theta_j$. Constant $\phi_{0j}=(1+2\kappa\eta_{0j}^2)^{1/2}/(2\kappa)$, and $\eta_{0j}$ is the unperturbed soliton amplitude (assumed order unity). Choice of the $(t,s)$ reference frame allows one to express perturbations in terms of various orders of $\kappa$. The analysis should allow XPM-induced refractive-index changes to modify soliton amplitude, width, and phase in a way that preserves energy flow. Simulations of soliton $j$ colliding with an unperturbed orthogonal beam show amplitude and phase slope perturbations of $O(\kappa)$, while soliton width remains unchanged. For arbitrary collision angles, width variation is assumed to be due to geometrical broadening [6], whereby $b_j(s)=\eta_{0j}\cos\delta\theta_j$ and $\delta b_j=O(\delta\vartheta_j^2)\leqslant O(\kappa^2)$. The evolution equation for $M_{tj}$ yields

$$\frac{d}{ds}(\delta\theta_j) = -2(1+h)\kappa\eta_{0j}^2\int_{-\infty}^{+\infty} dt|u_{3-j}(t,s)|^2\,\mathrm{sech}^2[\eta_{0j}(t+t_{0j})]\tanh[\eta_{0j}(t+t_{0j})]. \tag{10}$$

Consideration of $M_{sj}$ provides an expression for $\delta a_j$ that, when combined with the energy flow requirement of $\delta a_j=-1/2\,\eta_{0j}d/ds(\delta\sigma_j)$, gives

$$\frac{d}{ds}(\delta\sigma_j) = (1+h)\kappa\eta_{0j}\int_{-\infty}^{+\infty} dt|u_{3-j}(t,s)|^2\,\mathrm{sech}^2[\eta_{0j}(t+t_{0j})], \tag{11}$$

where, as with Eq. (10), only terms up to $O(\kappa)$ have been retained.

Figure 2(a) shows the magnitude of the trajectory phase shift $\Delta$, for both coherent and incoherent interactions, obtained from this approximate analytical approach. An approximate solution is first obtained by considering the interaction of soliton $j$ with an unperturbed soliton $u_{3-j}^0(t,s)$. Results are then refined iteratively using the earlier values of $t_{0j}(s)$ in the equations. Predictions are in good qualitative and quantitative agreement with the full numerical results. Figures 2(b)–2(d) give a detailed account of the evolution of soliton $j$ parameters when soliton $3-j$ remains unperturbed. Results from the adiabatic perturbation approach (points) are compared with those from the full NLH equation (1) (lines).

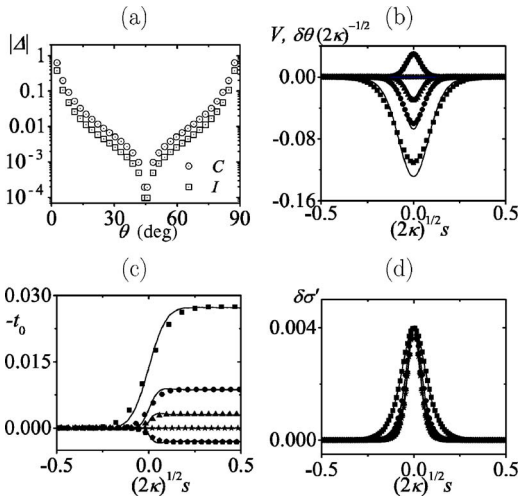


FIG. 2. (a) Magnitude of the trajectory shift obtained using the adiabatic perturbation method for coherent (C) and incoherent (I) interactions. Comparison of the evolution of (b) soliton transverse velocity, (c) soliton position, and (d) soliton phase variation, obtained from the numerical integration of Eq. (3) (lines) and the adiabatic perturbation method (points) for interaction angles 15° (squares), 25° (circles), 35° (triangles), 45°, (stars) and 55° (pentagons). In all cases, $\kappa=0.001$.

Excellent agreement is found between theoretical prediction and the numerical solution in all cases.

In summary, we have extended the theory of spatial Kerr soliton collisions to include arbitrary interaction angles. Both numerical and analytical investigations have also been undertaken. In particular, significant radiation generation arising from counterpropagating coherent solitons, predicted in Ref. [4], is found to occur only for near-exact alignment of beams. Soliton robustness is reported for all intermediate-angle collision geometries. Our approach and results, arising from a generic modification to the linear wave operator, are also expected to have implications for other solitons (e.g., vector and algebraic) and for solutions of other wave equations (e.g., involving higher dimensions and modified nonlinearity).

## ACKNOWLEDGMENTS

The authors wish to acknowledge support from MCyT and FEDER, grant number TIC2003-07020 and Junta de Castilla y León, project number VA083A05.

[1] G. Stegman and M. Segev, Science **286**, 1518 (1999).
[2] V. E. Zakharov and A. B. Shabat, Sov. Phys. JETP **34**, 62 (1972).
[3] J. P. Gordon, Opt. Lett. **8**, 596 (1983).
[4] O. Cohen, R. Uzdin, T. Carmon, J. W. Fleischer, M. Segev, and S. Odoulov, Phys. Rev. Lett. **89**, 133901 (2002).
[5] P. Chamorro-Posada, G. S. McDonald, and G. H. C. New, J. Opt. Soc. Am. B **19**, 1216 (2002).
[6] P. Chamorro-Posada, G. S. McDonald, and G. H. C. New, J. Mod. Opt. **45**, 1111 (1998).
[7] P. Chamorro-Posada, G. S. McDonald, and G. H. C. New, J. Mod. Opt. **47**, 1877 (2000).
[8] P. Chamorro-Posada and G. S. McDonald, Opt. Lett. **28**, 825 (2003).
[9] K. Marinov, D. I. Pushkarov, and A. Shivarova, *Soliton-Driven Photonics* (Kluwer Academic Publishers, New York,

2001), Vol. II/31, p. 293.
[10] A. Ciattoni, C. Conti, E. DelRe, P. Di Porto, B. Crosignani, and A. Yariv, Opt. Lett. **27**, 734 (2002).
[11] B. Crosignani, A. Yariv, and S. Mookherjea, Opt. Lett. **29**, 1254 (2004).
[12] A. Ciattoni, B. Crosignani, S. Mookherjea, and A. Yariv, Opt. Lett. **30**, 516 (2005).
[13] M. Lax, W. H. Louisell, and W. B. McKnight, Phys. Rev. A **11**, 1365 (1975).
[14] S. Chi and Q. Guo, Opt. Lett. **20**, 1598 (1995).
[15] A. W. Snyder, D. J. Mitchell, and Y. Chen, Opt. Lett. **19**, 524 (1994).
[16] E. Granot, S. Sternklar, Y. Isbi, B. Malomed, and A. Lewis, Opt. Lett. **22**, 1290 (1997).
[17] M. J. Ablowitz, G. Giondinni, S. Chakravrty, R. B. Jenkins, and J. R. Sauer, J. Opt. Soc. Am. B **14**, 1788 (1997).
[18] P. Chamorro-Posada, G. S. McDonald, and G. H. C. New, Opt. Commun. **192**, 1 (2001).
[19] A. Hasegawa and Y. Kodama, *Solitons in Optical Communications* (Oxford University Press, Oxford, 1995), Chap. 5, p. 75.